Generalized Simulated Annealing Studies on Structures and Properties of Ni_n ($n = 2-55$) Clusters

Y. Xiang, D. Y. Sun, and X. G. Gong*

Institute of Solid State Physics, Academia Sinica, 230031-Hefei, P. R. China

Received: August 19, 1999; In Final Form: November 29, 1999

With the generalized simulated annealing algorithm (GSA), the structures and properties of Ni_n ($n = 2-55$) clusters have been studied. We find that besides the icosahedral-like structure, the structures of Ni clusters can be decahedral-like or fragments of the fcc crystal. The clusters with $n = 13, 38, 55$ are found to be very stable. With modification of the effective coordination number model, the calculated ionization potentials of Ni clusters are in good agreement with the experimental data. The dynamical simulations show that the clusters with a closed-compact inner core have a high vibrational frequency mode, while the disordered clusters show some low vibrational frequency modes.

I. Introduction

The atomic clusters show many interesting physical properties which could have potential applications. However, the structure is the key ingredient to understanding these properties. Unfortunately, direct experimental determination of the atomic structure of small clusters is extremely difficult. Only some indirect methods have to be used in detecting the structure of a cluster. For example, for simple metal clusters, negative ion photoelectron spectroscopy can provide structural information.[1] The structures of some Ni clusters were probed by the flow-reactor approach, which is one of the most powerful techniques up to now.[2−5] The work of Riley and co-workers provided information about the structures of Ni_n clusters; however, in the size range $n = 29-48$, only one structural assignment was given because of a large number of possible geometries.[4] So, theoretical studies on the structures of clusters are still necessary, because they can give possible candidates for the lowest energy structure.[6−17]

Although ab initio methods, such as Hartree−Fock[7,8,13] and the density functional method,[6,10] can be used to study the structural properties of clusters with the total energy minimization, they are confined to limited atomic configurations in searching for the lowest energy structure. For clusters with a large number of atoms, classical optimization methods combined with a well-chosen empirical potential are still widely used.[18,19] Many algorithms, such as the simplex, the conjugate gradient relaxation, the steepest descent, and the Monte Carlo, are introduced into the structural optimization of clusters. With the annealing technique, the molecular dynamics (MD) method can be used to find the global energy minimum of clusters. However, for big clusters with a very large number of local minima, the efficiency of these methods becomes limited and the systems are usually trapped in a local energy minimum.

Among various theoretical algorithms, the simulated annealing method is believed to be the key to finding the global minimum of a complicated system.[20] Due to the inherent statistical nature of the simulated annealing, in principle local minima can be hopped much more easily than with many other methods. S. Kirkpatrick et al.[20] and Szu et al.[21] proposed the classical simulated annealing (CSA) and the so-called fast simulated annealing (FSA) methods, respectively. Recently, the generalized simulated annealing (GSA) based on the Tsallis generalized statistics has been proposed.[22−27]

In this paper we first apply the Stariolo−Tsallis form of GSA to a more realistic physical system, the nickel clusters, to determine the structures of Ni_n clusters ($n = 2-55$), in which the interatomic potentials are modeled by the Sutton−Chen version of FS potential.[28,29] With the obtained structures, the structural properties and some physical properties of Ni clusters are studied in detail.

The rest of the paper is organized as follows. In section II, we briefly present the GSA method and the interatomic potential for Ni used in this paper. Section III consists of results and discussion. The conclusion is presented in section IV.

II. GSA Method and Interatomic Potential

According to Tsallis,[22] generalized statistics can be built from the generalized entropy

$$s_q = k\frac{1 - \sum p_i^q}{q - 1} \tag{1}$$

where q is a real number and s_q tends to the information entropy

$$s = -k\sum p_i \ln p_i \tag{2}$$

equation when $q \to 1$. Maximizing the Tsallis entropy with the constraints

$$\sum p_i = 1 \qquad \sum p_i^q \epsilon_i = \text{const} \tag{3}$$

where ϵ_i is the energy spectrum, the generalized probability distribution is found to be

$$p_i = \frac{[1 - (1 - q)\beta\epsilon_i]^{1/1-q}}{z_q} \tag{4}$$

* Corresponding author. E-mail address: gong@theory.issp.ac.cn.

10.1021/jp992923q CCC: $19.00
Published on Web 02/24/2000

where z_q is the generalized partition function. This distribution becomes the Gibbs−Boltzman distribution where q tends to 1.

CSA and FSA can be generalized according to the Tsallis statistics within a unified picture. It is the so-called generalized simulated annealing algorithm (GSA),[22−24] which uses a somewhat distorted Cauchy−Lorentz visiting distribution whose shape is controlled by the parameter q_v:

$$g_{q_v}(\Delta x(t)) \propto \frac{[T_{q_v}(t)]^{-D/3-q_v}}{\left[1+(q_v-1)\frac{(\Delta x(t))^2}{[T_{q_v}(t)]^{2/3-q_v}}\right]^{1/q_v-1+D-1/2}} \quad (5)$$

q_v also controls the rate of cooling:

$$T_{q_v}(t) = T_{q_v}(1)\frac{2^{q_v-1}-1}{(1+t)^{q_v-1}-1} \quad (6)$$

T_{q_v} is the visiting temperature.

A generalized Metropolis algorithm for the acceptance probability is used:

$$p_{q_a} = \min\{1,[1-(1-q_a)\beta\Delta E]^{1/1-q_a}\} \quad (7)$$

where $\beta = 1/kT_{q_a}$, q_a is the same as the above q. For $q_a < 1$, zero acceptance probability is assigned to the case if

$$[1-(1-q_a)\beta\Delta E] < 0 \quad (8)$$

When $q_v = 1$ and $q_a = 1$, GSA recovers CSA. When $q_v = 2$ and $q_a = 1$, GSA recovers FSA. When $q_v > 2$, the cooling is faster than that of CSA and FSA. Because it has a large possibility for long jumps, the possibility of finding the global minimum with GSA is larger than that with FSA and CSA.

In the present studies, we choose the initial temperature with which the acceptance probability is about 86%. q_v and q_a are set to 2.62 and −5, respectively. To accelerate the convergence, we set the acceptance temperature equal to the visiting temperature divided by time steps, i.e., $T_{q_a} = T_{q_v}/t$. Our tests show that this simple technique works as well as our previous technique, which makes q_a decrease linearly with the steps.[25] For each initial configuration, we perform GSA until the visiting temperature reaches 0.01, and then a conjugate gradient minimization scheme is used for a short refinement. For each cluster, we have randomly chosen 1000 initial configurations; the obtained lowest-energy structure is considered as the ground-state structure.

The FS potential, which is regarded as one of the best potentials for transition metals,[30−33] is used to model the atomic interaction in Ni_n clusters. The Sutton−Chen version of this potential has the form

$$V = \epsilon\sum_i\left[\frac{1}{2}\sum_{j\neq 1}\left(\frac{a}{r_{ij}}\right)^n - c\rho_i^{1/2}\right] \quad (9)$$

where

$$\rho_i = \sum_{j\neq 1}\left(\frac{a}{r_{ij}}\right)^m \quad (10)$$

r_{ij} is the distance between the atoms i and j, a is the lattice constant, c is a dimensionless parameter, ϵ is the parameter with dimension of energy, and m and n are integers. The square root term in the attractive part of the potential accounts for many-body interaction. The parameters in the above equation for Ni are: $a = 3.52$ Å, $c = 39.432$, $\epsilon = 1.5707 \times 10^{-2}$ eV, $m = 6$, and $n = 9$. As shown by Nayak et al.,[34] the structures of small Ni clusters predicted by this potential are in good agreement with ab initio results.

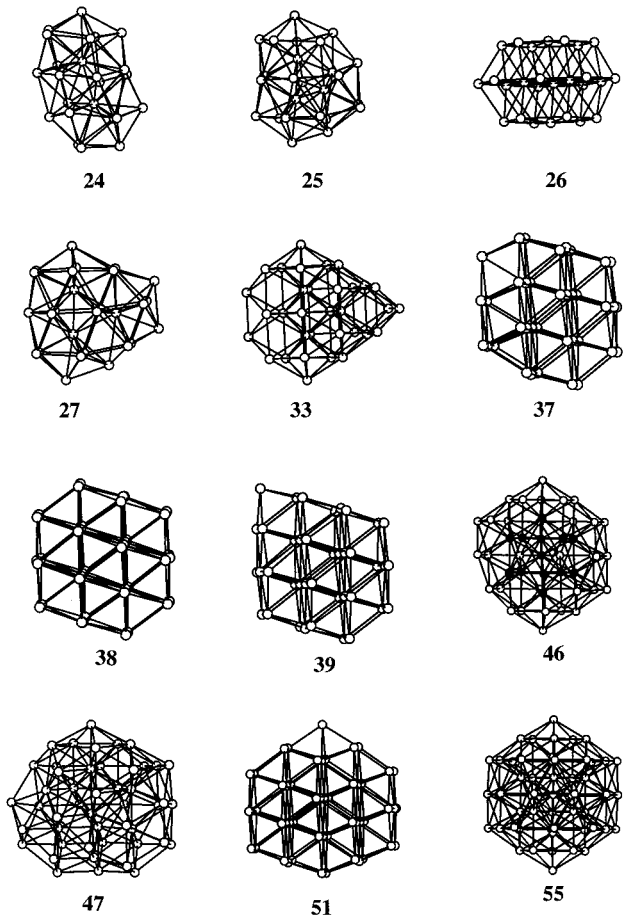

Figure 1. Atomic structures of Ni_n clusters.

III. Results and Discussion

With the ground state of Ni_n clusters obtained by GSA, structural properties, such as the average interatomic distance and average coordination number, are studied. The structural stability of the cluster has also been studied. Based on the modified effective coordination number model, we have also calculated the ionization potentials changing with the cluster size, and the vibrational spectra are obtained from molecular dynamics simulations.

III. 1 Geometries and Structural Properties. The ground state of Ni_n clusters are in agreement with available experimental[2−5] and theoretical[34] data, which indicate that the GSA method is efficient for exploring the structures of clusters. Structures of a few selected Ni clusters are shown in Figure 1.

From $n = 9$ to 25, the structures of clusters are more or less icosahedron-like. Ni_{24} and Ni_{25} can be roughly considered as a triple icosahedron plus one atom and two atoms, respectively (see Figure 1), which is in agreement with the structure proposed by Riley and co-workers.[5] Instead of a polyicosahedron proposed by Riley, the structure of Ni_{26} is found to be a fcc fragment with D_{3h} symmetry. We can see that Ni_{26} consists of three pieces of fcc(111) surfaces, which have 7, 12, and 7 atoms, respectively.

In the size range $n = 27-36$ (except $n = 33$), although these clusters do not have any ordered structures, most of their

structures can be constructed from small clusters ($n \leq 13$) with some face or edge sharing. For instance, Ni_{27} is found to be composed of Ni_{10}, Ni_{11}, and a hexagonal bipyramid.

The structure of Ni_{33} is found to be a decahedron. Its main part, as shown in Figure 1, is a pentagonal bipyramid with four atoms along the 5-fold axis, which is capped by 14 atoms. In the size range $n = 37-39$, it is interesting to find that the fcc-like structure favors the energy. The emergence of the fcc-like structure indicates the invalidity of the usual conception that all the clusters tend to adopt icosahedral structures. The structure of Ni_{37} is similar to a fcc fragment composed of four parallel arranged fcc(111) faces, as can be seen in Figure 1. The structure of Ni_{38} is found to be a fcc fragment and composed of four parallel arranged pieces of fcc(111) faces, which is in agreement with the recent experiment of Riley and co-workers.[4] Similar to Ni_{38}, Ni_{39} is also a fcc fragment, which can be obtained by adding an atom to Ni_{38}.

In the size range $n = 40-51$, the icosahedron, the decahedron, and fcc fragments appear alternately. For example, the structures of $Ni_{46,47}$ are icosahedral-like (Figure 1), but the structures of $Ni_{45,48}$ are decahedral-like. Similar to Ni_{37}, the structures of $Ni_{50,51}$ are fcc fragments with a stacking fault.

From $n = 52$ to $n = 55$, the clusters have the icosahedral structure and a perfect icosahedron is formed up to $n = 55$.

From the structural results presented above, we can see that, around $n = 13$ ($n = 9-25$) and $n = 55$ ($n = 52-55$), the structures of clusters are icosahedral-like. In going from the 13-atom icosahedron to the 55-atom icosahedron, fcc-like structures around $n = 38$ appear, which is in agreement with the recent experiment of Riley and co-workers.[4] However, the clusters between show very complicated structures. The present results show that the usual conception that all the metallic clusters tend to adopt icosahedral structures in not very large sizes is not valid for the case of Ni clusters.

To look into the structural properties in more detail, we first define the average interatomic distance in a cluster as:

$$\langle R \rangle = \frac{1}{n}\sum_i R_i \tag{11}$$

where R_i is the distance between the ith atom and its nearest neighbor. The average coordination number in a cluster is calculated by:

$$CN = \frac{1}{n}\sum_i C(i) \tag{12}$$

where $C(i)$ is the coordination number of the ith atom. We consider an atom j to be the neighbor of atom i if their distance R_{ij} is smaller than a cutoff 2.52 Å, 4% longer than the bond length in bulk.

The upper panel of Figure 2 shows the average interatomic distance. It increases monotonically with size until $n = 9$, but exhibits oscillations for larger clusters. The average interatomic distance of Ni_{55} is 2.357 Å, which is still 5% shorter than the nearest neighbor distance in bulk Ni. It is interesting to note that although the main trend of the average interatomic distance is to increase, peaks have appeared at Ni_{26}, Ni_{33}, Ni_{38}, and around Ni_{50} whose structures are either fcc fragments or decahedral-like with relatively longer interatomic distances as compared with the icosahedral structure. The fluctuations from $n = 39$ to $n = 50$ also indicate the alternate appearance of the fcc fragment, icosahedral-like structure, and decahedral-like structure.

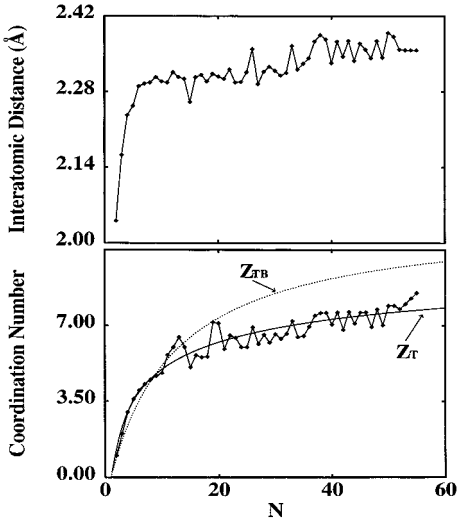

Figure 2. Upper panel, the average interatomic distance as a function of cluster size. Those clusters with fcc or decahedral structures, such as Ni_{26}, Ni_{33}, Ni_{38}, and Ni_{50}, have large average interatomic distance. Lower panel, the average coordination number as a function of cluster size. Line with dots, calculated data from the structure of clusters. Dashed line, Bhatt's empirical formula (Z_{TB}); solid line, our empirical formula (Z_T). The disagreement between the calculated values and the results from Bhatt's formula becomes significant for large clusters.

The average coordination numbers evolving with the cluster size, plotted in the lower panel of Figure 2, show no sign of the convergence to the bulk value. This can be easily understood if one notices that most of atoms in the clusters are at surface. Even for $n = 55$ there are only 13 inner atoms, and another 32 atoms are surface atoms; their average coordination numbers do not exceed 9. Bhatt et al. gave an approximate formula to describe the average coordination number Z_{TB} of the clusters:[35]

$$Z_{TB}(n) = \frac{n-1}{1+\frac{n-1}{12}} \tag{13}$$

Z_{TB} changing with the cluster size is also plotted in Figure 2. Obviously, this simple formula cannot give a satisfactory result, because it underestimates coordination number for small clusters and overestimates the coordination number for large clusters. To get a more accurate average coordination number, we give an empirical Z_T, as follows:

$$Z_T(n) = \frac{n-1}{1+\frac{n-1}{12}+b\times\frac{n-a}{n}\times(n-1)^c} \tag{14}$$

We find that Z_T, with the parameters $a = 8.762$, $b = 0.097$, and $c = 0.73$, can fit well to our calculated coordination number of Ni clusters, which is also shown in Figure 2. Comparing Z_T with Z_{TB}, we can see that both Z_T and Z_{TB} converge to 12 for n equal to infinite; however, Z_T converges much more slowly.

III.2 Stability and Ionization Potentials. To study the stability of clusters, we calculate the evolution of the binding energy E_b and the energy difference in adding an atom to the preceding cluster ΔE, which are defined by

$$E_b(n) = -\frac{E(n)}{n} \tag{15}$$

$$\Delta E(n) = E(n-1) - E(n) \tag{16}$$

where $E(n)$ is the total energy of a cluster with n atoms. In the

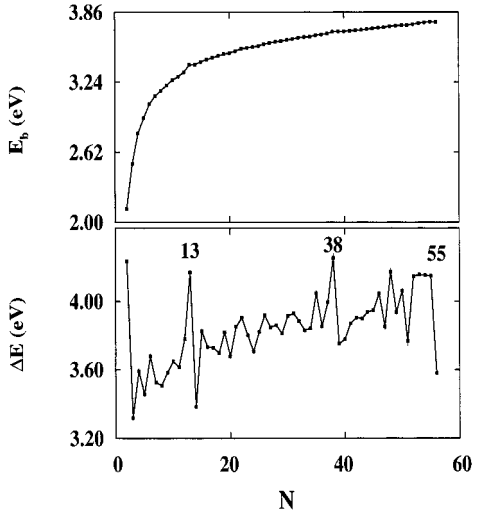

Figure 3. The binding energy (upper panel) and the energy difference in adding an atom (lower panel) as a function of cluster size. From the peaks in the lower panel, Ni_{13}, Ni_{38}, and Ni_{55} can be identified as the very stable clusters.

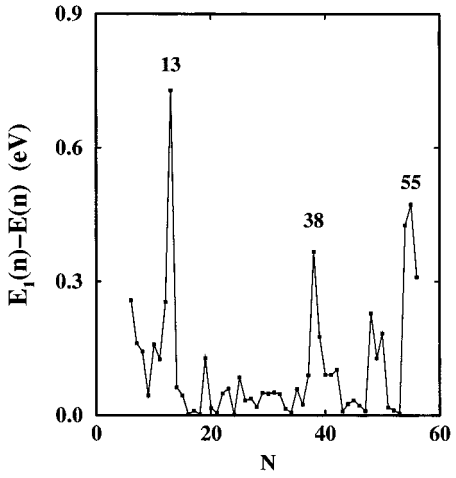

Figure 4. The energy difference between the ground state and its closest isomer. The peaks at $n = 13, 38, 55$ indicate that the structures of those clusters are stable.

limit of a very large cluster, E_b and ΔE should converge to the cohesive energy of the bulk. The difference of E_b (ΔE) to the bulk cohesive energy is a signature for the convergence of cluster properties to the bulk.

The binding energy E_b as a function of cluster size is plotted in the upper panel of Figure 3. Binding energy increases monotonically with size. However, up to Ni_{55}, the binding energy (3.77 eV) is still much lower than the cohesive energy of the solid (4.44 eV), which indicates that the convergence to the bulk is still far away.

The energy difference ΔE, plotted in the lower panel of Figure 3, shows the high stability of Ni_{13}, Ni_{38}, and Ni_{55}. Odd−even alternation can be observed until Ni_7, and this trend disappears for large clusters. Thirteen, 38, and 55 can be identified as magic numbers of Ni clusters.

The total energy difference $E_1(n)-E(n)$ can provide the information on the structure stability for the cluster, where $E_1(n)$ is the total energy of the lowest energy isomer obtained in the GSA optimization. Since the structural transition from ground-state structure to the isomer could strongly depend on $E_1(n)-E(n)$, the small $E_1(n)-E(n)$ could make the cluster fluctuate from one structure to another. The smaller $E_1(n)-E(n)$ is, the less stable the structure is. On the other hand, the large $E_1(n)-E(n)$ will make the cluster stable with the ground-state structure. Figure 4 shows $E_1(n)-E(n)$ obtained for the studied Ni clusters. We can see that peaks at $n = 13, 38, 55$ suggest that the structures of these clusters could be stable, the same as that predicted from ΔE.

It is interesting to calculate the ionization potential which can be measured by the experiment. For Na_n, K_n, etc., the classical conducting spherical droplet (CSD) model[36−38] can give good results that are in close agreement with experimental values. But when this model was applied to the transition metal clusters such as Ni_n, Co_n, and Fe_n, the deviation from the experimental results was large.[39,40] Even with ab initio methods, it is also difficult to get a good agreement between experimental and theoretical results; usually a difference as large as 0.5 eV could be possible.[34,42] So, even a simple model study can help to understand the physics of clusters.

Recently Zhao et al. have developed an effective coordination number (ECN) model for calculating ionization potentials of clusters:[41]

$$I_n = I_0 - (I_0 - W) \times \left(\frac{Z_s}{Z_b}\right)^{1/2} \tag{17}$$

where Z_s and Z_b are the average coordination number of surface atoms and bulk, respectively; I_0 is the first ionization potential of an atom; and W is the work function of the solid. An empirical formula of Z_s is

$$Z_s = \frac{Z_{TB}(n) - 12(1 - f(n))}{f(n)} \tag{18}$$

with $f(n) = 1.36 \times n^{-0.15}$.

As a matter of fact, in a cluster, all atoms mix together and form common electronic bands. Because all the atoms in the cluster contribute to the ionization potential, considering only surface atoms is not suitable. It would be better to replace Z_s with the average effective coordination number Z_T; in this way, we get our empirical formula for the ionization potential of the Ni cluster:

$$I_n = I_0 - (I_0 - W) \times \left\{\frac{n-1}{12 \times \left[1 + \frac{n-1}{12} + b \times \frac{n-a}{n} \times (n-1)^c\right]}\right\}^{1/2} \tag{19}$$

where $a = 8.762$, $b = 0.097$, and $c = 0.73$.

Figure 5 shows the ionization potentials versus the size of clusters, comparing with experimental data and model calculations. We can see that the effective coordination number model, based on our obtained structures, can give a correct trend for the ionization potentials of Ni clusters, which suggests that the model is reasonable for the transition metal clusters. However, the simple Z_s model shows large errors, especially for large clusters. These results suggest that the effective coordination number model can predict the right trend for the ionization potential of an Ni cluster, but using a correct average coordinate number is necessary.

III.3 Vibrational Spectra of Ni_n Clusters. Figure 6 shows the vibrational spectra of Ni_n clusters ($n = 2-55$) calculated from velocity auto-correlation function by performing molecular dynamics simulations at 80 K. We get a vibrational frequency for the dimmer to be 355 cm^{-1}, which is closer to the experimental value of 329 cm^{-1} [43] than that obtained by Garzon et al.[44]

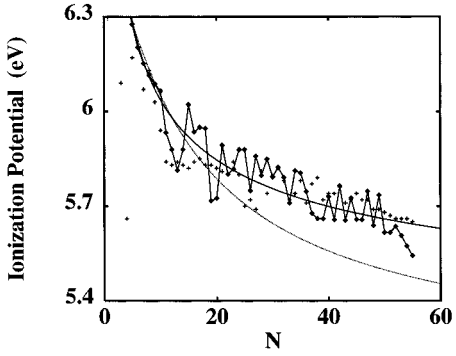

Figure 5. Ionization potentials calculated from the modified effective coordination number model. Cross dots, experimental data; line with dots, data from the average coordination number model. Solid line, data from eq 19. Dashed line, data from simple surface coordination number formula. The results from our empirical formula are in good agreement with experimental data.

The symmetry of the clusters can be reflected in the vibrational spectrum: the higher the symmetry, the more discrete the spectra. From Figure 6, the high discretion of vibrational spectra can be observed for Ni_{13} and Ni_{55}, whose structures are an icosahedron with I_h symmetry. Since the structure of Ni_4 is a tetrahedron with T_d symmetry and the structures of Ni_6 and Ni_{38} are an octahedron or a truncated octahedron, respectively, both of which have O_h symmetry, these clusters also show a certain degree of discretion. The discretion degree of other clusters is much lower, which indicates the lower symmetry of these clusters.

Some clusters show a high frequency around 11−12 THz, which can be observed from Figure 6. The high-frequency mode in the vibrational spectra for the clusters containing only a few atoms, such as Ni_2 and Ni_3, can be attributed to the small average bond length. The frequency mode moves to the lower band when the cluster size increases to $n = 8$. However, the high-frequency mode appears again for Ni_{12-15}, Ni_{19-21}, and Ni_{52-55}. By analyzing the corresponding atomic structure of these clusters, we find that all these clusters have a very compact inner core. For instance, although both Ni_{46} and Ni_{47} have an icosahedral-like structure, Ni_{46} has a high-frequency mode and Ni_{47} has not. This is because Ni_{46} has a compact core, whereas Ni_{47} is more defective and does have a compact core.

The appearance of the low-frequency modes for some clusters (n = 16−17, 27−31, 40) with quite disordered structures has been observed. This could happen if, in these clusters, some of atoms were very weakly bonded to the cluster. The similar emergence of the low-frequency mode in nanocrystal particles has recently been addressed by Stuhr[45] and Kara.[46]

IV. Conclusions

In summary, our studies show that GSA is an efficient method for exploring the structures of atomic clusters. The obtained lowest-energy structures of Ni_n (n = 2−55) clusters are in agreement with the available experimental and theoretical results. Besides the icosahedral structures reported before, Ni_n clusters with the decahedral-like structures and the fcc fragments have been found. In particular, the structure of the Ni_{38} cluster is found to be a truncated octahedron, which is in good agreement with the recent experiment. By analyzing the energy difference between the ground state and its closest isomer, we can conclude that structures of n = 13, 38, and 55 with a high symmetry are very stable, which is also confirmed by the binding energy and their differentials.

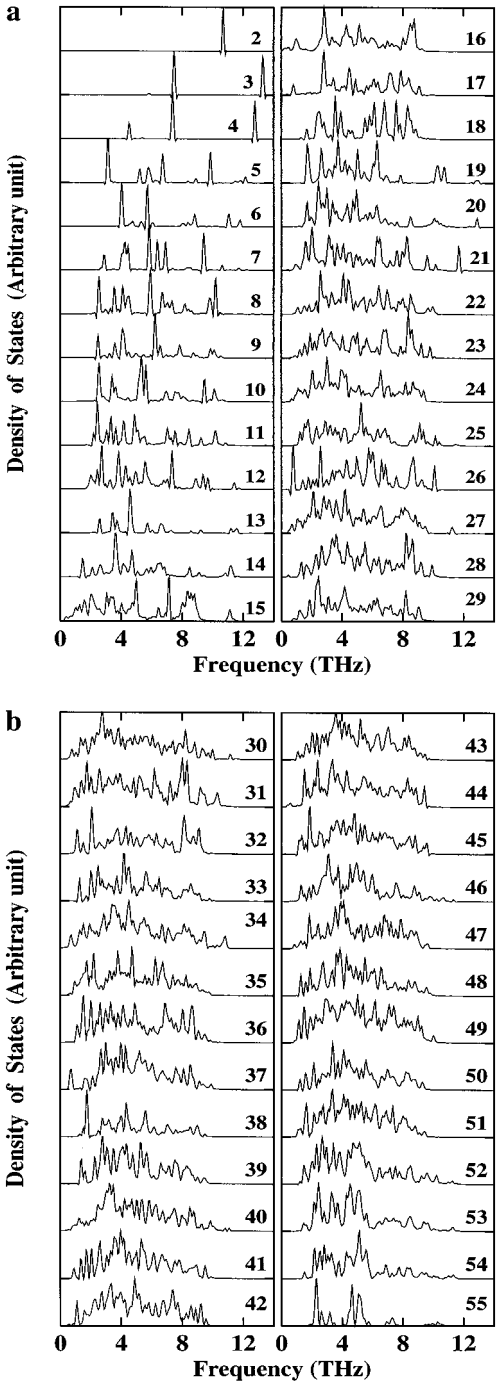

Figure 6. Vibration spectra of Ni_n clusters. (a), n =2−29; (b), n = 30−55.

By modifying the effective coordination number model, the ionization potential predicted by our empirical formula is in better agreement with the experimental data than the previous empirical formula. These results indicate that the simple model can give a correct trend of ionization potentials changing with size, but the correct calculation of the average coordination number is necessary. We have also identified that the local compact structure in the cluster causes appearance of a high-frequency vibration mode, and the disordered structure can lead to the emergence of the low-frequency modes.

Acknowledgment. X.Y. acknowledges W. Fan, M. Z. Li, and S. Y. Wang for the stimulating discussions. This work is partially supported by NNSF of China, Panden Project (973), and CAS project.

References and Notes

(1) Sarkas, H. W.; Arnold, S. T.; Handricks, J. H.; Bowen, K. H. *J. Chem. Phys.* **1995**, *102*, 2653. Schulze Icking-Konet, G.; Handschuh, H.; Gantefor, G.; Eberhardt, W. *Phys. Rev. Lett.* **1996**, *76*, 1047.

(2) Parks, E. K.; Zhu, L.; Ho, J.; Riley, S. J. *J. Chem. Phys.* **1994**, *100*, 7206.

(3) Parks, E. K.; Riley, S. J. *Z. Phys. D: At., Mol. Clusters* **1995**, *33*, 59.

(4) Parks, E. K.; Niemann, G. C.; Kerns, K. P.; Riley, S. J. *J. Chem. Phys.* **1997**, *107*, 1861.

(5) Parks, E. K.; Zhu, L.; Ho, J.; Riley, S. J. *J. Chem. Phys.* **1995**, *102*, 7377.

(6) Harris, J.; Jones, R. O. *J. Chem. Phys.* **1979**, *70*, 830.

(7) Basch, H.; Newton, M. D.; Moskowitz, J. *J. Chem. Phys.* **1980**, *73*, 4492.

(8) Tomonari, M.; Tatewaki, H.; Nakamura, T. *J. Chem. Phys.* **1986**, *85*, 2875.

(9) Bonacic-Koutecky, V.; Fantucci, P.; Koutecky, J. *Chem. Rev.* **1991**, *91*, 1035.

(10) Mlynarski, P.; Salahub, D. R. *J. Chem. Phys.* **1991**, *95*, 6050.

(11) Rao, B. K.; Jena, P.; Ray, A. K. *Phys. Rev. Lett.* **1996**, *76*, 2878.

(12) Rosch, N.; Ackermann, L.; Pacchioni, G. *Chem. Phys. Lett.* **1992**, *199*, 275.

(13) Pou-Amerigo, R.; Merchan, M.; Nebot-Gil, I.; Malmqvist, P. A.; Boss, B. O. *J. Chem. Phys.* **1994**, *101*, 4893.

(14) Castro, M.; Salahub, D. R. *Phys. Rev. B.* **1993**, *47*, 10955.

(15) Ballone, P.; Jones, R. O. *Chem. Phys. Lett.* **1995**, *233*, 632.

(16) Reuse, F. A.; Khanna, S. N. *Chem. Phys. Lett.* **1995**, *234*, 77.

(17) Cai, Z. X.; Mahanti, S. D.; Antonelli, A.; Khanna, S. N.; Jena, P. *Phys. Rev. B* **1992**, *46*, 7841.

(18) Jellinek, J.; Garzon, I. L. *Z. Phys. D: At., Mol. Clusters* **1991**, *20*, 239. Guvenc, Z. B.; Jellinek, J. *Z. Phys. D: At., Mol. Clusters* **1993**, *26*, 304. Lopez, M. J.; Jellinek, J. *Phys. Rev. A.* **1994**, *50*, 1445.

(19) Uppenbrink, J.; Wales, D. J. *J. Chem. Phys.* **1992**, *96*, 8520; *J. Chem. Phys.* **1993**, *98*, 5720.

(20) Kirkpatrick, S.; Gelatt, C. D., Jr.; Vecchi, M. P. *Science* **1983**, *220*, 671.

(21) Szu, H.; Hartley, R. *Phys. Lett. A* **1987**, *122*, 157.

(22) Tsallis, C. *J. Stat. Phys.* **1988**, *52*, 479.

(23) Tsallis, C.; Stariolo, D. A. *Generalized Simulated Annealing. Physica A* (in press).

(24) Hansmann, U. H. E. *Phys. A* **1997**, *242*, 250.

(25) Xiang, Y.; Sun, D. Y.; Fan, W.; Gong, X. G. *Phys. Lett. A.* **1997**, *233*, 216.

(26) Xiang, Y.; Sun, D. Y.; Gong, X. G. (to be published).

(27) Serra, P.; Stanton, A. F.; Kais, S.; Bleil, R. E. *J. Chem. Phys* **1997**, *106*, 7170.

(28) Finnis, M. W.; Sinclair, J. E. *Philos. Mag.* **1984**, *50*, 45.

(29) Sutton, A. P.; Chen, J. *Philos. Mag. Lett.* **1990**, *61*, 139.

(30) Todd, B. D.; Lynden-Bell, R. M. *Surf. Sci* **1993**, *281*, 191.

(31) Frenken, J. W. M.; Smeenk, R. G.; Van der Veen, J. F. *Surf. Sci.* **1983**, *135*, 147.

(32) Adams, D. L.; Petersen, L. E.; Sorensen, C. S. *J. Phys. C.* **1985**, *18*, 1753.

(33) Demuth, J. E.; Marcus, P. M.; Jespen, D. W. *Phys. Rev. B* **1975**, *11*, 1460.

(34) Doye, J. P. K.; Wales, D. J. *New J. Chem.* **1998**, *22*, 733. Nayak, S. K.; Khanna, S. N.; Rao, B. K.; Jena, P. *J. Phys. Chem. A* **1997**, *101*, 1072. Reddy, B. V.; Nayak, S. K.; Khanna, S. N.; Rao, B. K.; Jena, P. *J. Phys. Chem. A* **1998**, *102*, 1748.

(35) Bhatt, B. N.; Rice, T. M. *Phys. Rev. B.* **1979**, *20*, 466.

(36) Wood, D. M. *Phys. Rev. Lett.* **1981**, *46*, 749.

(37) Perdew, J. P. *Phys. Rev. B* **1988**, *37*, 6175.

(38) Makov, G.; Nitzan, A.; Brus, L. E. *J. Chem. Phys.* **1988**, *88*, 5076.

(39) Knickelbein, M. B.; Yang, S. H.; Riley, S. J. *J. Chem. Phys.* **1990**, *93*, 94.

(40) Parks, E. K.; Klots, T. D.; Riley, S. J. *J. Chem. Phys.* **1990**, *92*, 3813.

(41) Zhao, J. J.; Han, M.; Wang, G. H. *Phys. Rev. B.* **1993**, *48*, 15297.

(42) Gong, X. G.; Zheng, Q. Q. *J. Phys.: Condens. Matter* **1995**, *7*, 2421.

(43) Morse, M. D. *Chem. Rev.* **1986**, *86*, 1049.

(44) Posada-Amarillas, A.; Garzon, I. L. *Phys. Rev. B* **1996**, *54*, 10362.

(45) Stuhr, U.; Wipf, H.; Anderson, K. H.; Hahn, H. *Phys. Rev. Lett.* **1998**, *81*, 1449.

(46) Kara, A.; Rahman, T. S. *Phys. Rev. Lett.* **1998**, *81*, 1453.